

## FEEDBACK FROM HIGH-MASS X-RAY BINARIES ON THE HIGH REDSHIFT INTERGALACTIC MEDIUM : MODEL SPECTRA

CHRIS POWER<sup>1,4</sup>, GILLIAN JAMES<sup>2</sup>, CELINE COMBET<sup>3</sup> & GRAHAM WYNN<sup>2</sup>

<sup>1</sup> International Centre for Radio Astronomy Research, University of Western Australia, 35 Stirling Highway, Crawley, WA 6009, Australia

<sup>2</sup> Department of Physics & Astronomy, University of Leicester, Leicester, LE1 7RH, UK

<sup>3</sup> Laboratoire de Physique Subatomique et de Cosmologie, Université Joseph Fourier Grenoble 1/CNRS/IN2P3/INPG, 53 avenue des Martyrs, 38026 Grenoble, France

<sup>4</sup> ARC Centre of Excellence for All-Sky Astrophysics (CAASTRO)

*ApJ, accepted 23/11/2012*

### ABSTRACT

Massive stars at redshifts  $z \gtrsim 6$  are predicted to have played a pivotal role in cosmological reionization as luminous sources of ultra-violet (UV) photons. However, the remnants of these massive stars could be equally important as X-ray luminous ( $L_X \sim 10^{38}$  erg s<sup>-1</sup>) high-mass X-ray binaries (HMXBs). Because the absorption cross section of neutral hydrogen decreases sharply with photon energy ( $\sigma \propto E^{-3}$ ), X-rays can escape more freely than UV photons from the star-forming regions in which they are produced, allowing HMXBs to make a potentially significant contribution to the ionizing X-ray background during reionization. In this paper, we explore the ionizing power of HMXBs at redshifts  $z \gtrsim 6$  using a Monte Carlo model for a coeval stellar population of main sequence stars and HMXBs. Using the archetypal Galactic HMXB Cygnus X-1 as our template, we propose a composite HMXB spectral energy distribution consisting of black-body and power-law components, whose contributions depend on the accretion state of the system. We determine the time-dependent ionizing power of a combined population of UV-luminous stars and X-ray luminous HMXBs, and deduce fitting formulae for the boost in the population's ionizing power arising from HMXBs; these fits allow for simple implementation of HMXB feedback in numerical simulations. Based on this analysis, we estimate the contribution of high redshift HMXBs to the present-day soft X-ray background, and we show that it is a factor of  $\sim 100 - 1000$  smaller than the observed limit. Finally, we discuss the implications of our results for the role of HMXBs in reionization and in high redshift galaxy formation.

*Subject headings:* galaxies: formation – X-rays: binaries – cosmology:theory

### 1. INTRODUCTION

There is strong and compelling observational evidence that the Universe underwent an “Epoch of Reionization” within the first  $\sim 1$  billion years after the Big Bang (e.g. Ouchi et al. 2010; Mesinger 2010; Shull et al. 2012; McGreer et al. 2011). During this period, the cosmic abundance of neutral hydrogen was “re-ionized” by a background of ionizing ultra-violet (UV) and X-ray radiation produced by the first generation of stars and galaxies (e.g. Barkana & Loeb 2007; Robertson et al. 2010). The precise nature of these sources remains an outstanding problem, but it can be argued reasonably that massive stars ( $M_* \gtrsim 8 M_\odot$ ) must have been important (e.g. Wise & Abel 2008; Wise 2012).

Massive stars have fleeting main sequence (MS) lives ( $\sim 10$  Myrs), but as extremely luminous sources of hydrogen-ionizing UV photons (see, for example, Schaerer 2003) they are expected to play a crucial role in reionizing the Universe (e.g. Wyithe & Loeb 2003; Sokasian et al. 2004; Wise & Abel 2008). However, their predicted contribution to reionization depends on the ease with which UV photons can escape into the intergalactic medium (IGM), which depends on various factors, principally the clumpiness of the IGM (e.g. Pawlik et al. 2009). However, testing such predictions observationally is inherently challenging and a

clear consensus as to what the sources of reionization are is yet to emerge. For example, observations of star-forming galaxies at redshifts  $7 \lesssim z \lesssim 10$  hint that implied star formation rates are insufficient to produce enough massive stars to reionize the Universe by  $z \simeq 6$ , without including a population of galaxies below the detection limits and relaxing assumptions about the escape fraction of ionizing photons and extrapolated star formation rates (e.g. Bunker et al. 2010; McLure et al. 2010; Finkelstein et al. 2010; González et al. 2010). In contrast, observations of high redshift galaxies also suggest that the star formation rate at  $z \sim 9$  could be as high as that at  $z=0$  (cf. Ishida et al. 2011) and that the observable population of galaxies between  $6 \lesssim z \lesssim 8$  can sustain a fully reionized IGM at  $z=6$  if the average escape fraction of ionizing photons is  $\sim 30\%$  (cf. Finkelstein et al. 2012; see also Bouwens et al. 2012). A similar conclusion is drawn by Kistler et al. (2009), who argue that a sufficient number of massive stars could have formed to reionize the Universe by using high-redshift gamma ray bursts as a proxy for the integrated star formation rate between  $6 \lesssim z \lesssim 8$ .

It is, however, worth noting that massive stars can continue to ionize during their post-MS lives, predominantly as sources of X-rays. Oh (2001) noted that X-ray emission from supernovae in star forming regions in the high-redshift Universe should be large and compara-

ble energetically to UV emission. The role of supernovae has been explored further by Johnson & Khochfar (2011) who examined how strong shocking of the ISM associated with supernovae leads to the production of ionizing photons with harder spectra and larger escape fractions than UV photons. They estimate that such X-rays can boost – briefly – the ionizing power of a massive star by  $\sim 10\%$ .

Glover & Brand (2003) considered not only X-rays from supernovae but also from X-ray binaries in their examination of the contribution of star formation to the build up of the high redshift X-ray background. As Justham & Schawinski (2012) have demonstrated in their recent study, X-ray binaries are likely to be important sources of feedback across cosmic time (see also Fragos et al. 2012). In particular, we expect this to be the case at early times; in Power et al. (2009) (hereafter P09) we explored how high mass X-ray binaries (HMXBs)\* in primordial globular clusters at high redshifts could boost the UV ionizing power of the cluster. We found that harder ionizing spectra combined with enhanced escape fractions for X-rays implied that HMXBs could be just as efficient at ionizing the IGM as their MS progenitors. Similar ideas have been explored in Mirabel et al. (2011) and Wheeler & Johnson (2011), in which the primary is a stellar mass black hole, as well as by McQuinn (2012) in his census of potential sources of reionization.

The analysis in P09 focused on the ionizing power of HMXBs in globular clusters because (i) the inferred ages of metal poor globular clusters imply that they formed at  $z \gtrsim 6$  (cf. Brodie & Strader 2006); (ii) the relationship between the initial mass functions (IMF) of stars and the dynamical evolution of clusters is well understood (cf. Vesperini & Heggie 1997); and (iii) the escape fraction for UV photons was likely to be large, assuming that globular clusters followed similar orbits then to the ones they follow now (cf. Ricotti 2002, who explored the ionizing power of massive stars in globular clusters). This last point is important because the large UV escape fraction allowed P09 to carry out a straightforward comparison of a globular cluster’s UV and X-ray ionizing power.

However, as noted in P09, HMXBs are likely to be a generic by-product of high mass star formation (cf. Helfand & Moran 2001), and should form as well in gas-rich galaxy discs as in young globular clusters. This is consistent with observations of star forming galaxies at  $z \lesssim 1$  that show that luminous compact X-ray sources – with properties mirroring those of HMXBs in our Galaxy – are good indicators of recent star formation activity (see Figure 10 of Mineo et al. 2012a and Figure 2 of Mineo et al. 2012b). In this paper, we extend the analysis presented in P09 to study HMXBs as generic sources of ionizing radiation. Here our focus is on refining our treatment of their spectral energy distribution. Rather than assuming a simple power-law form for the HMXB spectrum (as we did in P09), we use the spectrum of Cygnus X-1, the archetypal Galactic HMXB (e.g. Remillard & McClintock 2006), as our template. We assess how this impacts on the ionizing power of a coeval stellar population over time and we

quantify how the ionizing luminosity of the population is boosted by the presence of HMXBs. Finally, we estimate the possible contribution of HMXBs to the present-day soft X-ray background, assuming both our new template spectrum and power-law spectra of the kind that have been used in previous studies (e.g. P09).

The structure of the remainder of this paper is as follows. In § 2 we describe our time-dependent Monte Carlo model for the spectral energy distribution of a coeval population of stars in which HMXBs are forming. In § 3 we present results for the time evolution of the ionizing power and spectral energy distribution of the population, and we quantify how HMXBs enhance the ionizing power of the stellar population. In § 4, we show that the X-ray luminosity produced in our model does not violate observed limits on the soft X-ray background. Finally, we summarize our results in § 5 and comment on their implications for cosmological reionization and high redshift galaxy formation.

## 2. METHODS

### 2.1. Modelling HMXBs in a Single Stellar Population

As in P09, we set up a Monte Carlo model of a stellar population, assumed to form in a single instantaneous burst, and follow the evolution of the massive stars over the first 250 million years, through their MS lives and into the HMXB phase. The main features of our model can be summarized as follows;

*THE MASSIVE STAR POPULATION:* We assume the IMF of Kroupa (2001) as our fiducial case, with stellar masses spanning the range  $0.01 \leq M_*/M_\odot \leq 100$ , but we also verify our results for the Salpeter (1955) and top-heavy Chabrier (2001) IMFs. All stars with  $M_* \geq 8M_\odot$  are assumed to form in binaries – these are the progenitor population from which the HMXBs are drawn. Initial binary parameters are assigned following Dray (2006) – that is, companion masses are drawn from a uniform distribution between  $0.01 \leq M_*/M_\odot \leq 100$  and orbital periods are distributed uniformly in logarithm between 1 and  $10^4$  days. Massive star lifetimes are estimated using the results of Marigo et al. (2001, 2003), Schaerer et al. (1993) and Meynet & Maeder (2000) for metallicities of  $Z = 0, 0.008$  and  $0.02$  (i.e. solar metallicity) respectively; we explore the  $Z = 0$  case in our results section.

*THE HMXB POPULATION:* We assume that HMXBs form from binaries in which the initial MS mass of the primary exceeds  $M_* \sim 8M_\odot$ , the threshold for neutron star formation (cf. Figure 1 of Heger et al. 2003a), and the donor (i.e. secondary) mass lies in the range  $M_* \geq 3M_\odot^\dagger$ . Once the primary goes supernova, we estimate the remnant mass using Figure 3 of Heger et al. (2003a). The binary will be disrupted if it loses more than half its mass in the supernova – which, for our fiducial Kroupa IMF, implies that approximately 30% of bi-

\* We assumed an initial primary mass of  $M_* \geq 8M_\odot$ .

<sup>†</sup> This donor mass is lower than the usual definition of HMXBs – donor OB stars (cf. Table 1 of Fabbiano 2006) with typical masses  $\gtrsim 10M_\odot$  (e.g. Justham & Schawinski 2012). However, it is reasonable to include these intermediate mass X-ray binaries because they are sufficiently luminous to contribute to the X-ray ionizing power of the stellar population and their MS lifetimes are of order  $\sim 10^8$  yrs.

aries survive, thereby setting an upper limit to the total number of HMXBs that can potentially form. Following P09, we draw a survival fraction  $f_{\text{sur}}$  of this  $\sim 30\%$  at random and consider them as HMXBs;  $f_{\text{sur}}$  captures the various uncertainties that prevent massive binaries from evolving into HMXBs. We assume that HMXBs are active until the companion star evolves off the main sequence and goes supernova.

We have noted already that the binaries that survive are more likely to host black holes than neutron stars, especially in low metallicity systems where the formation rate of HMXBs in which the primary is a black hole could be a factor of  $\sim 10$  higher than at Solar metallicity (cf. Linden et al. 2010; Justham & Schawinski 2012). There is also observational evidence that the black hole mass is likely to be larger in lower metallicity systems (cf. Crowther et al. 2010). This should, in principle, shape our HMXB luminosity function (cf. Dray 2006). However, we make the simplifying assumption to draw HMXB luminosities from a Weibull distribution with a peak luminosity of  $L_X \sim 10^{38} \text{ erg s}^{-1}$  but capped such that they do not accrete at super-Eddington rates; this sets an upper limit of approximately  $L_X \simeq 1.26 \times 10^{38} (M/M_\odot) \text{ erg s}^{-1}$  on the luminosity of an HMXB with primary mass  $M$ . This approach gives a distribution that is consistent with the luminosities of compact X-ray sources in nearby galaxies whose X-ray binary populations are dominated by HMXBs (cf. Figure 1 of Gilfanov et al. 2004); see P09 for further discussion of this point.

## 2.2. Spectral Energy Distribution & Time Dependence

We split the spectral energy distribution of the stellar population into two components:

*MAIN SEQUENCE (MS) STARS:* Each star is assumed to radiate as a black body with an effective temperature of

$$T_{\text{eff}} = \left( \frac{L_*}{4\pi R_*^2 \sigma_{\text{SB}}} \right)^{1/4} \quad (1)$$

where  $R_*/R_\odot = (M_*/M_\odot)^{0.8}$  is stellar radius and  $\sigma_{\text{SB}}$  is the Stefan-Boltzmann constant. Stellar luminosity  $L_*$  is assumed to follow a mass-luminosity relation of the form

$$\frac{L_*}{L_\odot} = \alpha \left( \frac{M_*}{M_\odot} \right)^\beta, \quad (2)$$

where  $\alpha$ , which governs the amplitude of the relation, and  $\beta$ , which governs its slope, are observed to depend on stellar mass (e.g. Henry 2004); their values and the stellar mass range in which they are applicable are summarized in Table 1.

Empirically there is a wealth of evidence that the rate at which stellar luminosity varies with mass ( $\beta = d \log L / d \log M$ ) decreases with increasing mass  $M_*$ . For example, Malkov (2007) find  $\beta \sim 4.1$  at  $M \sim 1 M_\odot$  to  $\beta \sim 3.2$  at  $M \sim 20 M_\odot$  (see their Table 6), while Vitrichenko et al. (2007) report that  $\beta \sim 2.76$  over the mass range  $20 \lesssim M/M_\odot \lesssim 50$ . Our values of  $\alpha$  and  $\beta$  provide a good approximation to the functional form presented in Malkov (2007) for stellar masses  $M_* \lesssim 50 M_\odot$ . Above  $50 M_\odot$  we must extrapolate because observationally inferred data are few; we assume that the relation

**Table 1**  
Adopted Mass-Luminosity Relation.

$M_{\text{min}}/M_\odot$	$M_{\text{max}}/M_\odot$	$\alpha$	$\beta$
0.5	3	0.8	4.5
3	10	1.8	3.6
10	20	5.8	3.1
20	50	25.8	2.6
50	100	100.0	2.3

is slightly shallower than it is below  $50 M_\odot$ . This is an uncertainty, but it has negligible effect on our results because relatively few stars are formed in this mass range and their lifetimes are short. We find that the mass-luminosity relation can be well approximated by a 2<sup>nd</sup>-order polynomial of the form,

$$\log L_*/L_\odot = c_0 + c_1 \log M_*/M_\odot + c_2 (\log M_*/M_\odot)^2. \quad (3)$$

Here the coefficients have the values  $c_0 = -0.04172$ ,  $c_1 = 4.4954$  and  $c_2 = -0.6041$ , and  $\log$  indicates logarithm base 10.

*HIGH MASS X-RAY BINARIES:* We model HMXB spectra using the archetypal Galactic HMXB Cygnus X-1 as our template. Cygnus X-1 is the brightest HMXB in the Galaxy and it has been studied in exquisite detail (see, for example, the recent review by Remillard & McClintock 2006). It consists of a black hole of mass  $8.7 \pm 0.8 M_\odot$  (Shaposhnikov & Titarchuk 2007) and a super-giant companion (HDE 226868). Its spectrum is observed to fluctuate between distinct low-hard and high-soft states, examples of which can be found in Gierliński et al. (1999).

- The low-hard state is characterized by a luminosity of  $L_{2-10\text{keV}} \sim 3 \times 10^{36} \text{ erg s}^{-1}$  and a hard power-law spectrum  $\propto E^{-\Gamma}$  with spectral index of  $\Gamma \sim 1.6-1.8$  (e.g. Gierliński et al. 1997, 1999).
- The high-soft state is characterized by luminosity roughly one order of magnitude higher and a strong black body component with  $kT \sim 0.5 \text{ keV}$  with soft power-law tail with  $\Gamma \sim 2.5$  (e.g. Dolan et al. 1977; Ogawara et al. 1982).

This suggests that we should adopt distinct spectral shapes for low-hard and high-soft states. However, we understand neither what sets the duration of these two states – for example, Cygnus X-1 is observed to be predominantly in its low hard state, but analogous systems such as LMC X-3 (Val-Baker et al. 2007) appear to spend more time in their high soft state – nor how the nature and duration of these states depend on factors such as metallicity. For this reason, we make the simplifying assumption that HMXB spectra do not vary in time and instead introduce a threshold in X-ray luminosity of  $10^{37} \text{ erg s}^{-1}$ , above (below) which a source is in a soft (hard) state. In particular, we model

- the low-hard state as a power-law of slope -0.8 between 2 – 10 keV, the energy range in which this spectrum profile is observed, and
- the high-soft state by a composite black body and power-law spectrum – the power-law has a slope -1.1 and is normalized such that the ratio between

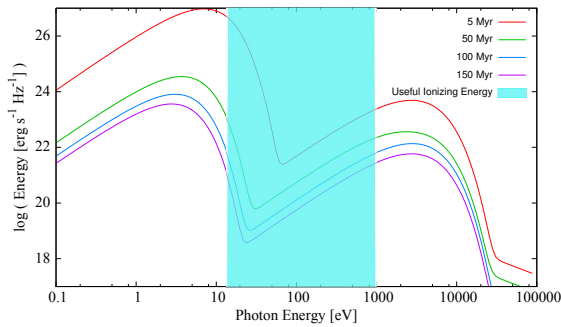


**Figure 1.** Spectra of the total energy output of the fiducial stellar population (i.e.  $N=10^6$ , Kroupa IMF,  $f_{\text{sur}} = 1$ ) after 5, 50, 100, and 150 Myrs (solid, long-, medium- and short-dashed curves respectively). The spectral shape derives from the stellar UV black body and the HMXB softer black body + harder power-law component, where we use the spectrum of Cygnus X-1 for our HMXB template.

the luminosities of the black body and power-law components matches that of Cygnus X-1, while the black body temperature is calculated by assuming  $(L_X/L_{\text{CygX-1}}) = (T/T_{\text{CygX-1}})^4$ .

### 3. RESULTS

In the following subsections, we show how the ionizing power of a stellar population formed in an instantaneous burst evolves over the first 150 Myrs after formation (§ 3.1). We compare and contrast results in the presence and absence of HMXBs and, where appropriate, we comment on the sensitivity of our results to the assumed value of the survival fraction ( $f_{\text{sur}}$ ) and our choice of IMF.

#### 3.1. Ionizing Power over Time

In Figure 1 we show the spectral energy distribution of the fiducial stellar population (i.e. Kroupa IMF,  $f_{\text{sur}} = 1$  and  $N=10^6$ ) as a function of time – a composite of MS stars, which we model individually as black bodies, and HMXBs, which we model as a combination of black bodies and power-law components. The amplitude of the black body corresponding to MS stars decreases with time, while its peak shifts to lower energies; this reflects the evolution of the most massive stars in the stellar population – which dominate the UV-luminosity – off the MS. Over the same period the amplitudes of both the black body and power-law components of the HMXBs decrease with time.

The same qualitative trends can be seen if we vary the IMF from Kroupa to Chabrier or Salpeter – there is a systematic increase (decrease) in the amplitude for the Chabrier (Salpeter) IMF, which reflects an increase (decrease) in the proportion of massive stars that form. If we vary the size of population between  $N=10^4$  to  $N=10^6$  the amplitude varies linearly with the size of population. Varying the survival fraction  $f_{\text{sur}}$  between 0.01 and 1 suppresses the amplitude of the HMXB black body and power-law contribution while leaving the black body contribution from the MS unchanged.

In Figure 2 we estimate how much of this energy (instantaneous in the upper panel, cumulative in the lower panel) is available to ionize neutral atomic hydrogen (HI) in the IGM as a function of time. We evaluate this by integrating the spectra plotted in Figure 1 between a lower limit of 13.6 eV, the minimum photon energy required to

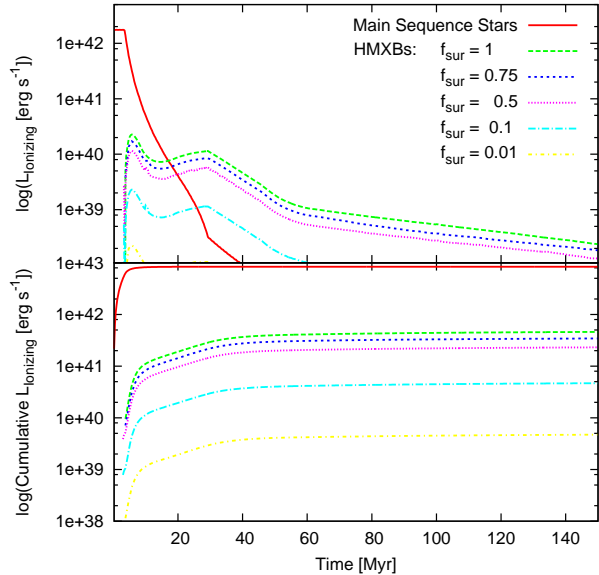


**Figure 2.** Time evolution of the instantaneous and cumulative ionizing power of a stellar population of  $N = 10^6$  stars and a Kroupa IMF (upper and lower panels respectively). Solid curves correspond to the contribution from MS stars only; curves of different line types correspond to the combined contribution of MS stars and HMXBs for five different values of the survival fraction  $f_{\text{sur}}$  with  $0.01 \leq f_{\text{sur}} \leq 1$ .

ionize atomic hydrogen, and an upper limit of  $E_{\text{lim}}$ , the energy above which atomic hydrogen becomes transparent to hard X-rays<sup>‡</sup>; for the redshift range we consider ( $z \gtrsim 6$ ),  $E_{\text{lim}} \gtrsim 1$  keV. Provided  $f_{\text{sur}} > 0.1$ , we find that HMXBs dominate the ionizing power of the stellar population after  $\sim 20$  Myrs.

Interestingly we note that the X-ray ionizing power shows a pronounced bump between  $20 \lesssim t \lesssim 40$  Myrs. This is an imprint of our definition of an HMXB as a binary system in which the mass of the primary must exceed  $\sim 8M_{\odot}$  at the end of its MS lifetime – the threshold for neutron star formation. Because the MS lifetime of an  $8M_{\odot}$  is  $\sim 25$  Myrs (cf. Marigo et al. 2001, 2003) and because statistically we expect more HMXBs to be drawn from stars close to this  $8M_{\odot}$  limit, we expect an excess in HMXBs to form around this time and to produce a bump in the ionizing power. After this time, HMXBs can no longer form and the ionizing power comes from a population that is in terminal decline.

We quantify how HMXBs enhance the ionizing power of the stellar population by measuring the boost factor  $f_{\text{HMXB}} = L_{\text{HMXB}}/L_{\text{MS}}$ , which compares the ionizing luminosity of the MS stars only ( $L_{\text{MS}}$ ) and of the combined MS stars and HMXBs ( $L_{\text{HMXB}}$ ). In Figure 3 we show how  $f_{\text{HMXB}}$  varies with time for a stellar population of  $10^6$  stars and  $f_{\text{sur}}=1$  assuming Kroupa, Salpeter and Chabrier IMFs respectively (solid curves, left to right panels). Because the ionizing power of the MS component declines sharply after  $\sim 10 - 20$  Myrs as the most massive stars end their lives,  $f_{\text{HMXB}}$  grows steadily with

<sup>‡</sup> As in P09, we estimate  $E_{\text{lim}}$  by requiring that  $\sigma(E_{\text{lim}}) = c^{-1}H(z)n_{\text{H}}(z)^{-1}$  where  $\sigma(E)$  is the ionization cross section of neutral hydrogen,  $H(z)$  is the Hubble parameter at redshift  $z$ ,  $n_{\text{H}}(z)$  is the mean number density of hydrogen and  $c$  is the speed of light.

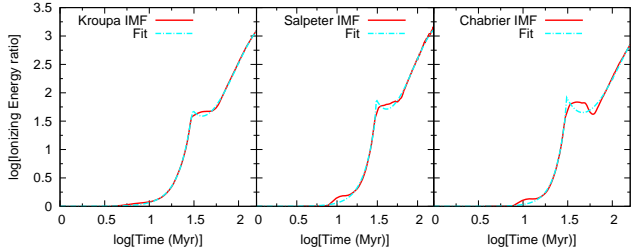


**Figure 3.** Time evolution of the boost factor  $f_{\text{HMXB}} = L_{\text{HMXB}}/L_{\text{MS}}$  for a stellar population of  $N = 10^6$  stars, a survival fraction  $f_{\text{sur}} = 1$  and a Kroupa, Salpeter and Chabrier IMFs (left, middle and right panels respectively). Dotted-dashed curves correspond to polynomial fits of the form given by Equation 4 with parameters given in Table 2.

**Table 2**  
Boost Factor  $f_{\text{HMXB}}$  Parameters.

IMF	$p$	$q$	$a$	$b$	$c$	$d$
Kroupa	7.85	6.73	54.2	-85.4	45.0	-7.61
Salpeter	6.53	6.82	66.2	-104	55.1	-9.40
Chabrier	0.852	8.23	46.8	-69.2	34.3	-5.42

time, peaking at  $f_{\text{HMXB}} \sim 1600$  after  $t \sim 180$  Myrs before dropping off abruptly. The dashed curves in Figure 3 show fits to the numerical results that agree to better than 10%. We fit the results with 2 formulae, below and above the bump at 30 Myr. These are given by

$$\log(f_{\text{HMXB}}) = \begin{cases} 10^{-5} p e^{q \log t} & t < 30 \\ a + b \log t + c(\log t)^2 + d(\log t)^3 & t > 30 \end{cases} \quad (4)$$

where  $t$  is population age in Myr, and are valid up to approximately 180 Myr, above which HMXB contribution falls rapidly to 0 (and  $f_{\text{HMXB}}$  drops to 1). The parameters  $p$ ,  $q$  and  $a$  to  $d$  are tabulated in Table 2.

#### 4. COSMIC SOFT X-RAY BACKGROUND

The Universe at  $z \gtrsim 6$  is effectively transparent to photons with energies  $\gtrsim 1$  keV. This means that hard photons remain unabsorbed by neutral hydrogen and so a hard X-ray background was built up in the early Universe that, through redshifting, contributes to the present day soft X-ray background (SXRb), the mean specific background intensity of soft X-rays. We wish to determine the contribution made to the SXRb by the HMXB population present at  $z \gtrsim 6$  and whether or not their contribution violates observed limits. Equivalent calculations have been performed by Dijkstra et al. (2004), Salvaterra et al. (2005) and Zaroubi et al. (2007) for mini-quasars in the early Universe. However, we adopt the approach of Dijkstra et al. (2012), who looked at the contribution of star-forming galaxies to both the soft and hard X-ray backgrounds from high redshift to the present day.

In what follows, we assume values of  $H_0 = 100h \text{ km s}^{-1} \text{ Mpc}^{-1}$  for the Hubble parameter with  $h=0.71$ ,  $\Omega_{\text{M}} = 0.266$  for the matter density parameter, and  $\Omega_{\Lambda} = 0.734$  for the dark energy density parameter (cf. Komatsu et al. 2011), and we take

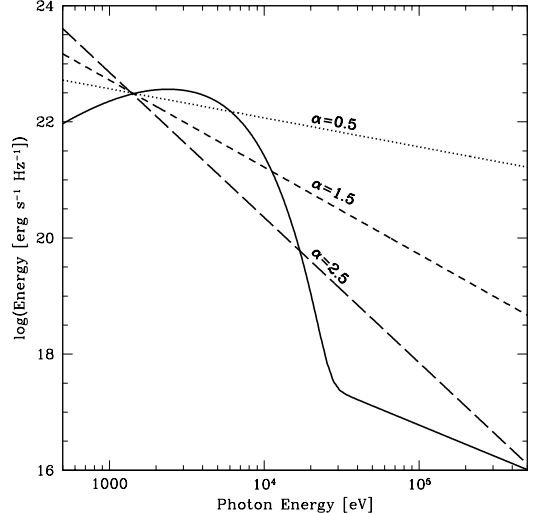


**Figure 4.** Comparison of the composite (i.e. black-body plus power-law) HMXB spectral energy distribution (solid curve) and possible power-law alternatives (with indices  $\alpha=0.5, 1.5, 2.5$ , corresponding to dotted, dashed and dotted-dashed curves respectively). The composite HMXB spectrum is as measured at  $t=50$  Myrs in Figure 1, while the power-law spectra are normalized such that the total energy emitted between 1 and 2 keV is the same for both the composite and power-law spectra.

as our observed limit on the SXRb the value of  $\sim 3.4 \pm 1.4 \times 10^{-13} \text{ erg s}^{-1} \text{ cm}^{-2} \text{ deg}^{-2}$  obtained by Hickox & Markevitch (2007) for the excess flux between 1–2 keV, which corresponds to hard X-rays at  $z \gtrsim 6$ . We estimate the contribution made by high redshift HMXBs to the observed SXRb by evaluating

$$\text{SXRb} = \frac{\Delta\Omega}{4\pi} \frac{c}{H_0} \int_6^{z_{\text{max}}} \frac{\dot{\rho}_* \mathcal{L}_X(z)}{(1+z)^2 \mathcal{E}(z)} dz, \quad (5)$$

where  $\Delta\Omega \sim 3 \times 10^{-4} \text{ sr deg}^{-2}$ ;  $c$  is the speed of light;  $z_{\text{max}}$  is the earliest (unknown) redshift at which HMXB formation proceeds;  $\mathcal{E}(z) = \sqrt{\Omega_{\text{M}}(1+z)^3 + \Omega_{\Lambda}}$ ;  $\dot{\rho}_*$  is the comoving star formation rate density in units of  $\text{M}_{\odot} \text{ yr}^{-1} \text{ Mpc}^{-3}$ ; and  $\mathcal{L}_X(z)$  is the “K-corrected” X-ray luminosity per unit star formation rate in the observed energy range  $X = E_1 - E_2$ .

For  $\dot{\rho}_*$  we explore four possibilities, spanning the range of potential star formation histories. We take (i) a fixed value of  $\dot{\rho}_*(z=6) \simeq 0.002 \text{ M}_{\odot} \text{ yr}^{-1} \text{ Mpc}^{-1}$ , as measured at  $z=6$  by Bunker et al. (2010); (ii) a fixed value of  $\dot{\rho}_*(z=6) \simeq 0.17 \text{ M}_{\odot} \text{ yr}^{-1} \text{ Mpc}^{-1}$ , as measured at  $z=6$  by Tanvir et al. (2012); (iii) a fixed value of  $\dot{\rho}_*(z=6) \simeq 0.02 \text{ M}_{\odot} \text{ yr}^{-1} \text{ Mpc}^{-1}$ , estimated at  $z=6$  using the functional form of Hopkins & Beacom (2006),

$$\dot{\rho}_*(z) = \frac{(u + vz)h}{1 + (z/w)^x}, \quad (6)$$

with parameters  $u=0.017$ ,  $v=0.13$ ,  $w=3.3$  and  $x=5.3$  from Cole et al. (2001); and (iv) a redshift-dependent value of  $\dot{\rho}_*$ , estimated using Equation 6.

For  $\mathcal{L}_X(z)$  we follow Dijkstra et al. (2012) and recast it as  $\mathcal{L}_X(z) = c_X K(z)$ . Here we assume the range of values for  $2.6 \leq c_X/10^{39} \text{ ergs}^{-1} (\text{M}_{\odot} \text{ yr}^{-1})^{-1} \leq 3.7$  measured by Mineo et al. (2012b) for compact resolved X-ray sources

in galaxies (lower limit) and unresolved galaxies in the Chandra Deep Field North and ultra-luminous infra-red galaxies (upper limit); and we calculate

$$K(z) = \frac{\int_{E_1(1+z)}^{E_2(1+z)} EF(E)dE}{\int_{0.5\text{keV}(1+z)}^{8\text{keV}(1+z)} EF(E)dE} \quad (7)$$

where  $F(E)$  represents the spectrum of a single HMXB,  $E_1=1$  keV and  $E_2=2$  keV. Examples of the spectra we consider are shown in Figure 4 – the solid curve corresponds to the cumulative spectrum derived from HMXBs in the fiducial stellar population described in §3, as measured at  $t=50$  Myrs<sup>§</sup>, while the dashed, dotted and dotted-dashed curves correspond to power-law spectra ( $\propto E^{-\alpha}$ ) that have been normalized such that the total energy emitted between 1 and 2 keV is the same for both composite and power-law spectra. The units are arbitrary – it is the shape, not the amplitude, that is important when evaluating Equation 7 – and it is worth noting how poorly simple power-law spectra approximate the shape of the more realistic composite spectrum.

In all cases we fix our lower bound in Equation 5 at  $z = 6$  and allow our upper bound  $z_{\text{max}}$  to vary between  $z = 20$  and  $z=50$ . This corresponds to a range in age of the Universe of between 48 and  $\sim 180$  Myrs old ( $z=50$  and  $20$  respectively), which is likely to bracket the redshifts when the first generation of dark matter halos were sufficiently massive to support cooling and subsequent star formation formed (cf. Figure 1 of Glover 2005). However, we note that our results are insensitive to  $z_{\text{max}}$  for the range of values that we consider.

Evaluating Equation (5), we find that the contribution of HMXBs to the soft X-ray background is of order  $\sim 5 \times 10^{-16}$  erg s<sup>-1</sup> cm<sup>-2</sup> deg<sup>-2</sup>, depending on what precisely is assumed for the star formation rate density and spectrum – roughly a factor of  $\sim 1000$  smaller than the observed limit of  $\sim 3.4 \times 10^{-13}$  erg s<sup>-1</sup> cm<sup>-2</sup> deg<sup>-2</sup> measured by Hickox & Markevitch (2007). In general, the higher the star formation rate density, the larger the contribution that is possible, because of our assumption that HMXB formation tracks (massive) star formation. If power-law spectra are adopted, we find that SXR  $\sim 2.15 \times 10^{-16}$  erg s<sup>-1</sup> cm<sup>-2</sup> deg<sup>-2</sup> for  $\alpha=0$  compared to  $\sim 11.4 \times 10^{-16}$  erg s<sup>-1</sup> cm<sup>-2</sup> deg<sup>-2</sup> for  $\alpha=2$ ; that is, the softer the spectrum, the larger the contribution HMXBs can make. Nevertheless, this contribution is still a factor of  $\sim 100$  smaller than the observed limit.

## 5. SUMMARY

There are compelling astrophysical reasons to expect that HMXBs, which are observed to be a natural by-product of massive star formation (e.g. Mineo et al. 2012a; Dijkstra et al. 2012), could be an important source of feedback in galaxy formation over cosmic time (e.g. Justham & Schawinski 2012). Because the cross section for photons to be absorbed by neutral hydrogen decreases strongly with energy as  $E_{\gamma}^{-3}$ , X-rays from HMXBs can effectively diffuse through the IGM and deposit their energy at relatively large distances from the

stellar population, in an act of non-local feedback (a similar effect is expected for mini-quasars; see, for example, Zaroubi & Silk 2005). This contrasts with lower energy UV photons, whose correspondingly larger absorption cross section means that they ionize the IGM in the vicinity of the stellar population, in an act of local feedback.

In this paper, we build on the work of Power et al. (2009) in which we examined the X-ray luminosity and effective ionizing power<sup>¶</sup> of a coeval population of stars and HMXBs at  $z \gtrsim 6$ .

- We have used the archetypal Galactic HMXB, Cygnus X-1, as our template for a more realistic HMXB spectrum. The form of this spectrum depends on the accretion state of the system and is a composite of black-body and power-law components.
- Using this new composite spectrum, we have quantified how HMXBs enhance the ionizing power of the stellar population by defining the boost factor  $f_{\text{HMXB}} = L_{\text{HMXB}}/L_{\text{MS}}$  (where  $L_{\text{MS}}$  and  $L_{\text{HMXB}}$  are the ionizing luminosities of a population of MS stars and a combined population of MS stars and HMXBs respectively) and characterizing and its variation with time. Because the ionizing power of the MS component declines sharply after  $\sim 10$ - $20$  Myrs as the most massive stars end their lives, we find that  $f_{\text{HMXB}}$  grows steadily with time before peaking at  $t \sim 100$  Myrs and after dropping off abruptly. This demonstrates the relatively long-lived nature of HMXBs as ionizing sources when compared to young massive stars on the MS.
- Finally, we have estimated the contribution of HMXBs to the soft X-ray background by assuming that HMXB formation is linked explicitly to the global star formation rate density, and we show that it does not violate observed limits. Depending on what is assumed for the star formation rate density, we estimate a contribution of  $\sim 5 \times 10^{-16}$  erg s<sup>-1</sup> cm<sup>-2</sup> deg<sup>-2</sup> if HMXB spectra are modelled as composite black-bodies and power-laws – roughly a factor of  $\sim 1000$  smaller than the observed limit of  $\sim 3.4 \times 10^{-13}$  erg s<sup>-1</sup> cm<sup>-2</sup> deg<sup>-2</sup> measured by Hickox & Markevitch (2007).

We do not compare the HMXB contribution to the ionizing X-ray background present during reionization to the contribution from other source populations, such as mini-quasars and accreting super-massive black holes, in this paper. Such a comparison has been carried out by McQuinn (2012) who concludes that HMXBs were likely to be a minor contributor to reionization. This may be the case – although the conclusion depends on the assumed spectral properties of the various sources considered, which in most cases are uncertain – but our work implies that HMXBs can have a significant impact on the ionization structure and heating rate of the IGM at

<sup>§</sup> We treat the unnormalized cumulative spectrum as indicative of the shape of a typical HMXB.

<sup>¶</sup> We made the simplifying assumption that an energetic X-ray photon can ionize multiple hydrogen atoms, and so treated secondary electrons that ionize hydrogen atoms as effective photons.

$z \gtrsim 6$ , extending the volumes of partially ionized hydrogen by factors of  $\gtrsim 1000$ . This will have a direct impact on the efficiency of galaxy formation by, for example, suppressing the collapse of gas onto low-mass dark matter halos (e.g. Machacek et al. 2003; Tanaka et al. 2012) and modifying the cooling rate of hot gas in galaxy halos (e.g. Cantalupo 2010). We will demonstrate this explicitly in a forthcoming paper (James et al., in preparation), in which we will use the more realistic composite spectrum in a radiative transfer calculation to assess the relative importance of such HMXB feedback in heating the high redshift IGM and the potential HMXB contribution to both cosmological reionization and galaxy formation in general.

## ACKNOWLEDGEMENTS

We thank the anonymous referee for their insightful report that has helped improve this paper. CP, GJ, CC and GW acknowledge the support of the theoretical astrophysics STFC rolling grant at the University of Leicester. Part of the research presented in this paper was undertaken as part of the Survey Simulation Pipeline (SSimPL; <http://www.astronomy.swin.edu.au/SSimPL/>). The Centre for All-Sky Astrophysics is an Australian Research Council Centre of Excellence, funded by grant CE11E0090.

## REFERENCES

- Barkana, R., & Loeb, A. 2007, *Reports of Progress in Physics*, 70, 627
- Bouwens, R. J., Illingworth, G. D., Oesch, P. A., et al. 2012, *ApJ*, 752, L5
- Brodie, J. P., & Strader, J. 2006, *ARA&A*, 44, 193
- Bunker, A. J., Wilkins, S., Ellis, R. S., et al. 2010, *MNRAS*, 409, 855
- Cantalupo, S. 2010, *MNRAS*, 403, L16
- Chabrier, G. 2001, *ApJ*, 554, 1274
- Cole S., et al., 2001, *MNRAS*, 326, 255
- Crowther, P. A., Barnard, R., Carpano, S., et al. 2010, *MNRAS*, 403, L41
- Delgado-Donate, E. J., Clarke, C. J., Bate, M. R., & Hodgkin, S. T. 2004, *MNRAS*, 351, 617
- Dijkstra, M., Haiman, Z., & Loeb, A. 2004, *ApJ*, 613, 646
- Dijkstra, M., Gilfanov, M., Loeb, A., & Sunyaev, R. 2012, *MNRAS*, 421, 213
- Dolan, J. F., Crannell, C. J., Dennis, B. R., Frost, K. J., & Orwig, L. E. 1977, *Nature*, 267, 813
- Dray, L. M. 2006, *MNRAS*, 370, 2079
- Fabbiano, G. 2006, *ARA&A*, 44, 323
- Finkelstein, S. L., Papovich, C., Gialalisco, M., et al. 2010, *ApJ*, 719, 1250
- Finkelstein, S. L., Papovich, C., Ryan, R. E., et al. 2012, *ApJ*, 758, 93
- Fragos, T., Lehmer, B., Tremmel, M., et al. 2012, *arXiv:1206.2395*
- Gierliński, M., Zdziarski, A. A., Done, C., et al. 1997, *MNRAS*, 288, 958
- Gierliński, M., Zdziarski, A. A., Poutanen, J., et al. 1999, *MNRAS*, 309, 496
- Gilfanov, M., Grimm, H.-J., & Sunyaev, R. 2004, *Nuclear Physics B Proceedings Supplements*, 132, 369
- Glover, S. C. O., & Brand, P. W. J. L. 2003, *MNRAS*, 340, 210
- Glover, S. 2005, *Space Sci. Rev.*, 117, 445
- González, V., Labbé, I., Bouwens, R. J., et al. 2010, *ApJ*, 713, 115
- Greif T. H., Springel V., White S. D. M., Glover S. C. O., Clark P. C., Smith R. J., Klessen R. S., Bromm V., 2011, *ApJ*, 737, 75
- Heger, A., Fryer, C. L., Woosley, S. E., Langer, N., & Hartmann, D. H. 2003a, *ApJ*, 591, 288
- Helfand, D. J., & Moran, E. C. 2001, *ApJ*, 554, 27
- Henry, T. J. 2004, *Spectroscopically and Spatially Resolving the Components of the Close Binary Stars*, 318, 159
- Hickox, R. C., & Markevitch, M. 2007, *ApJ*, 671, 1523
- Hopkins, A. M., & Beacom, J. F. 2006, *ApJ*, 651, 142
- Ishida, E. E. O., de Souza, R. S., & Ferrara, A. 2011, *MNRAS*, 418, 500
- Johnson, J. L., & Khochfar, S. 2011, *ApJ*, 743, 126
- Justham, S., & Schawinski, K. 2012, *MNRAS*, 423, 1641
- Kaplan, S. A., & Pikelner, S. B. 1970, Cambridge: Harvard University Press, 1970,
- Kistler, M. D., Yüksel, H., Beacom, J. F., Hopkins, A. M., & Wyithe, J. S. B. 2009, *ApJ*, 705, L104
- Komatsu, E., Smith, K. M., Dunkley, J., et al. 2011, *ApJS*, 192, 18
- Kroupa, P. 2001, *MNRAS*, 322, 231
- Linden, T., Kalogera, V., Sepinsky, J. F., et al. 2010, *ApJ*, 725, 1984
- Machacek, M. E., Bryan, G. L., & Abel, T. 2003, *MNRAS*, 338, 273
- Malkov, O. Y. 2007, *MNRAS*, 382, 1073
- Marigo, P., Girardi, L., Chiosi, C., & Wood, P. R. 2001, *A&A*, 371, 152
- Marigo, P., Chiosi, C., & Kudritzki, R.-P. 2003, *A&A*, 399, 617
- McGreer, I. D., Mesinger, A., & Fan, X. 2011, *MNRAS*, 415, 3237
- McLure, R. J., Dunlop, J. S., Cirasuolo, M., et al. 2010, *MNRAS*, 403, 960
- McQuinn, M. 2012, *MNRAS*, 426, 1349
- Mesinger, A. 2010, *MNRAS*, 407, 1328
- Meynet, G., & Maeder, A. 2000, *A&A*, 361, 101
- Mineo, S., Gilfanov, M., & Sunyaev, R. 2012a, *MNRAS*, 419, 2095
- Mineo, S., Gilfanov, M., & Sunyaev, R. 2012b, *MNRAS*, 426, 1870
- Mirabel, I. F., Dijkstra, M., Laurent, P., Loeb, A., & Pritchard, J. R. 2011, *A&A*, 528, A149
- Ogawara, Y., Mitsuda, K., Masai, K., et al. 1982, *Nature*, 295, 675
- Oh, S. P. 2001, *ApJ*, 553, 499
- Ouchi, M., Shimasaku, K., Furusawa, H., et al. 2010, *ApJ*, 723, 869
- Pawlik, A. H., Schaye, J., & van Scherpenzeel, E. 2009, *MNRAS*, 394, 1812
- Pen, U.-L. 1999, *ApJS*, 120, 49
- Power, C., Wynn, G. A., Combet, C., & Wilkinson, M. I. 2009, *MNRAS*, 395, 1146
- Remillard, R. A., & McClintock, J. E. 2006, *ARA&A*, 44, 49
- Ricotti, M. 2002, *MNRAS*, 336, L33
- Robertson, B. E., Ellis, R. S., Dunlop, J. S., McLure, R. J., & Stark, D. P. 2010, *Nature*, 468, 49
- Salpeter, E. E. 1955, *ApJ*, 121, 161
- Salvaterra, R., Haardt, F., & Ferrara, A. 2005, *MNRAS*, 362, L50
- Schaerer, D., Charbonnel, C., Meynet, G., Maeder, A., & Schaller, G. 1993, *A&AS*, 102, 339
- Schaerer, D. 2003, *A&A*, 397, 527
- Shaposhnikov, N., & Titarchuk, L. 2007, *ApJ*, 663, 445
- Shull, J. M., & van Steenberg, M. E. 1985, *ApJ*, 298, 268
- Shull, M., Harness, A., Trenti, M., & Smith, B. 2012, *ApJ*, 747, 100
- Sokasian, A., Yoshida, N., Abel, T., Hernquist, L., & Springel, V. 2004, *MNRAS*, 350, 47
- Tanaka, T., Perna, R., & Haiman, Z. 2012, *MNRAS*, 425, 2974
- Tanvir, N. R., Levan, A. J., Fruchter, A. S., et al. 2012, *ApJ*, 754, 46
- Val-Baker, A. K. F., Norton, A. J., & Negueruela, I. 2007, *The Multicolored Landscape of Compact Objects and Their Explosive Origins*, 924, 530
- Vesperini, E., & Heggie, D. C. 1997, *MNRAS*, 289, 898
- Vitrichenko, E. A., Nadyozhin, D. K., & Razinkova, T. L. 2007, *Astronomy Letters*, 33, 251
- Wheeler, J. C., & Johnson, V. 2011, *ApJ*, 738, 163
- Wise, J. H. 2012, *arXiv:1201.4820*
- Wise, J. H., & Abel, T. 2008, *ApJ*, 684, 1
- Wyithe, J. S. B., & Loeb, A. 2003, *ApJ*, 588, L69
- Zaroubi, S., & Silk, J. 2005, *MNRAS*, 360, L64
- Zaroubi, S., Thomas, R. M., Sugiyama, N., & Silk, J. 2007, *MNRAS*, 375, 1269